PHYSICAL REVIEW A **71**, 043810 (2005)

Statistical properties of the Stokes signal in stimulated Brillouin scattering pulse compressors

I. Velchev
Department of Radiation Physics, Fox Chase Cancer Center, 333 Cottman Avenue, Philadelphia, Pennsylvania 19111, USA

W. Ubachs
Laser Centre, Department of Physics and Astronomy, Vrije Universiteit, De Boelelaan 1081, 1081 HV Amsterdam, The Netherlands
(Received 18 October 2004; published 12 April 2005)

Spontaneous scattering noise is incorporated as a build-up source in a fully transient stimulated Brillouin scattering (SBS) model. This powerful simulation tool is successfully applied for a quantitative investigation of the fluctuations in the output pulse duration of SBS pulse compressors. The predictions of this model are experimentally verified in a two-stage SBS compressor.

DOI: 10.1103/PhysRevA.71.043810 PACS number(s): 42.65.Es, 42.65.Re, 42.60.By

I. INTRODUCTION

Pulse compression through stimulated scattering is an idea originally developed in the late 1960s [1], when it was noted that backward Raman scattering could efficiently (50-70 %) compress a seeded redshifted Stokes pulse. After more than one decade of research, aimed at high-peak intensities for laser ignition in nuclear fusion, a more suitable candidate for compression of powerful pulses emerged. Offering phase-conjugation, high quantum efficiency, and high gain, stimulated Brillouin scattering (SBS) was first applied in the early 1980s [2] and soon after replaced stimulated Raman scattering as the gain medium of choice for pulse compressors. Since then, the enormous potential of SBS has been realized, and commercial lasers employing internal pulse compression are now available.

Due to its robustness and maintenance-free operation, the SBS pulse compression scheme is nowadays an essential tool in many research labs. Its applications cover a variety of experiments ranging from the generation of narrowband tunable extreme ultraviolet pulses for precision spectroscopic studies [3] to the production of short powerful pulses for lifetime measurements [4]. The potential this technique offers can be utilized in future XUV lithographic sources, which currently rely on nanosecond laser pulses [5].

Unless injection-seeded, the backscattered wave in stimulated Brillouin scattering builds up from noise. The pump wave is scattered from thermally excited density fluctuations and, as a result, the Stokes signal has an inherent randomness in its phase and intensity. Although the random component is small compared to the stimulated (coherent) contribution, its effect on the conjugated signal is a measurable quantity. In the case of SBS pulse compressors, these fluctuations manifest themselves as a spread in the pulse duration and peak intensity. This highly undesirable effect may hinder the performance of an optical setup, and may ultimately limit the signal-to-noise ratio in an experiment, utilizing compressed pulses. In this article, we demonstrate the predictive power of a simulation tool, based on a transient SBS model [6] incorporating spontaneous scattering as a build-up source. In our experimental investigation, the pulse-to-pulse fluctuations in a two-stage SBS pulse compressor are quantified and the relationship with the thermal noise (through spontaneous Brillouin scattering) is established.

II. EXPERIMENT AND DATA ANALYSIS

The experimental arrangement for statistical investigation of a SBS pulse compressor is presented in Fig. 1. An injection-seeded and frequency-doubled Nd:YAG laser (Quanta Ray GCR 330) provides Fourier-transform limited Gaussian 5 ns pulses with energy 300 mJ/pulse. The linearly polarized beam passes through a polarization beam splitter and enters a two-stage generator-amplifier SBS pulse compressor [7,8]. We use distilled and filtered (down to 0.5 μm particle size) water as the SBS active medium. In the conditions of our experiment ($\lambda = 532$ nm and room temperature), the acoustic waves in water have a (phonon) lifetime of $\tau_p = 1/\Gamma_B = 295$ ps and a Stokes shift of $\Omega_B = 7.42$ GHz. Due to the scalar nature of Brillouin scattering (mediated by phonons), the polarization state of the reflected light is not changed and the compressor setup acts as a mirror for the polarization state, whereas the wavefront is phase conjugated. In addition to the nearly 100% energy efficiency of the compressor itself, this peculiarity of the SBS interaction allows for an extremely efficient pulse extraction by means of a quarter-wave plate (QWP). The total losses in our setup are measured to be of the order of 30%, due to the large number of optical surfaces. Losses can be further reduced by the use of a single-cell setup [9]. Our study, however, is focused on the statistical properties of the compressed pulse. Therefore, no further steps were made to improve the energy efficiency. Furthermore, in order to avoid saturation of the streak camera (Hadland IMACON), an attenuator is inserted in the

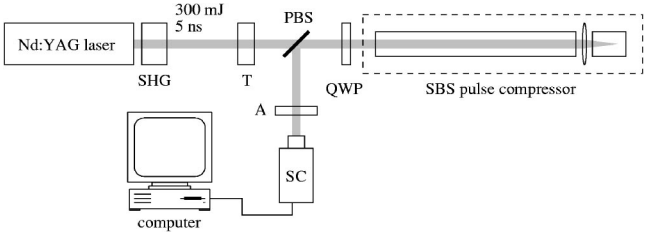

FIG. 1. The experimental setup: SHG, second harmonic generation crystal; T, telescope; PBS, thin-film polarization beam splitter; QWP, quarter-wave plate (Fresnel rhomb); A, attenuator; SC, streak camera.

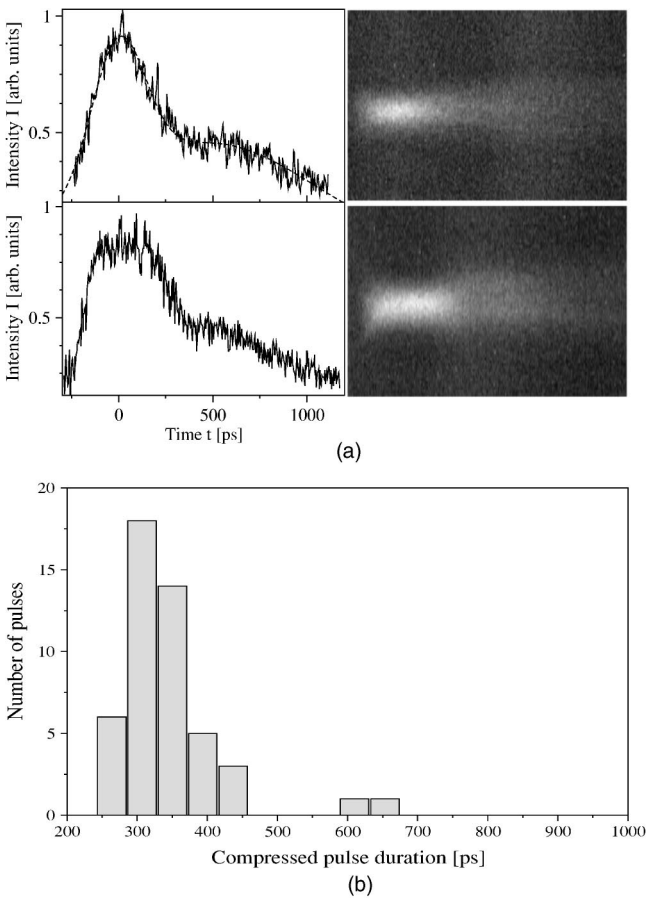

FIG. 2. Streak camera traces and intensity graphs (a) of a typical compressed pulse (upper panel) and an occasional longer pulse (lower panel) at the output of an SBS pulse compressor in water. (b) A histogram of the measured compressed pulse durations.

beam path (see Fig. 1). The streak camera ramp synchronization as well as the image accumulation are both properly triggered by the laser.

The pump laser pulse duration in our experiment is an order of magnitude longer than the phonon lifetime in the compressor. Therefore, the output pulse duration is expected to be limited by τ_p [2,6,10]. Since the backscattered SBS pulse builds up from light scattered off density fluctuations, the thermal noise in the generator cell will inevitably manifest itself through a measurable spread in the output pulse duration, which in turn results in pulse-to-pulse peak intensity fluctuations. In Fig. 2(a), two exemplary streak camera traces are presented. In the upper panel, the typical short output pulse of approximately 300 ps duration (full width at half maximum) is shown. On rare occasions, pulses with longer duration are recorded as well, as seen in the lower panel of Fig. 2(a). The measured pulse shapes exhibit a sharp peak followed by a wide plateau in the tail. This peculiar pulse shape is clear evidence that the pump pulse is completely depleted at the front of the backscattered pulse, while the trailing edge experiences no significant amplification. Using an adjustable telescope (T) before the compressor, the beam diameter and divergence are controlled in a manner that eliminates the relaxation oscillations.

A series of 58 pulses were measured; every streak camera trace was analyzed and the pulse duration histogram is presented in Fig. 2(b). The mean of the distribution is found at 320 ps and confirms the value estimated previously from the phonon lifetime under the conditions of the experiment. Pulses of shorter as well as longer durations are seen in the graph, contributing to a standard deviation of 42 ps. Fluctuations of such magnitude may be undesirable for some applications. Therefore, it is important that the spread can be estimated and taken into account during the design stage of an experiment. In the following section, we present a numerical method capable of accurately predicting the expected pulse-to-pulse fluctuations in a SBS compressor.

III. NUMERICAL MODEL AND DISCUSSION

When a pulse is compressed to a pulse duration comparable with the phonon lifetime in the medium, the transient nature of the process has to be taken into account. In an earlier work [6], we have shown that the transient evolution of the pulse envelope is governed by the following system of coupled partial differential equations:

$$\frac{\partial}{\partial t}A_1(z,t)+\frac{c}{n}\frac{\partial}{\partial z}A_1(z,t)=-i\alpha\frac{c}{n}\varrho(z,t)A_2(z,t), \tag{1a}$$

$$\frac{\partial}{\partial t}A_2(z,t)-\frac{c}{n}\frac{\partial}{\partial z}A_2(z,t)=-i\alpha\frac{c}{n}\varrho^*(z,t)A_1(z,t), \tag{1b}$$

$$\varrho(z,t)=\frac{1}{\sqrt{2\pi}}\int_{-\infty}^{t}g(t-\tau)A_1(z,\tau)A_2^*(z,\tau)d\tau, \tag{1c}$$

where A_1 and A_2 are the slowly varying amplitudes of the pump and Stokes pulses, respectively; c/n is the speed of light in water, $\alpha=g_B\Gamma_B/2$ is the effective transient gain parameter (g_B is the small-signal Brillouin gain), and

$$g(t)=\begin{cases}0, & t<0\\ \dfrac{-\sqrt{2\pi}\Omega_B e^{-(\Gamma_B/2)t}}{\sqrt{\Omega_B^2-\dfrac{\Gamma_B^2}{4}}}e^{i\Omega_B t}\sin\left(\sqrt{\Omega_B^2-\dfrac{\Gamma_B^2}{4}}t\right), & t\geqslant 0\end{cases} \tag{2}$$

is the time-dependent gain function [6].

By introducing a *propagation operator* $\hat{P}=(c/n)(\partial/\partial z)$ and a *nonlinearity operator* $\hat{N}=-i\alpha(c/n)\varrho\cdot$, Eqs. (1) can be rewritten in vector form,

$$\frac{\partial}{\partial t}\begin{pmatrix}A_1\\A_2\end{pmatrix}=\left(\begin{bmatrix}0 & \hat{N}\\ -\hat{N}^* & 0\end{bmatrix}+\begin{bmatrix}-\hat{P} & 0\\ 0 & \hat{P}\end{bmatrix}\right)\begin{pmatrix}A_1\\A_2\end{pmatrix}. \tag{3}$$

We solve the system Eq. (3) using a split-step method, in which the propagation operator acts first, followed by the nonlinearity, as depicted in Fig. 3(a). A detailed description of the numerical procedure can be found in Ref. [6]. We have chosen the spatial discretization step Δz equal to the propa-

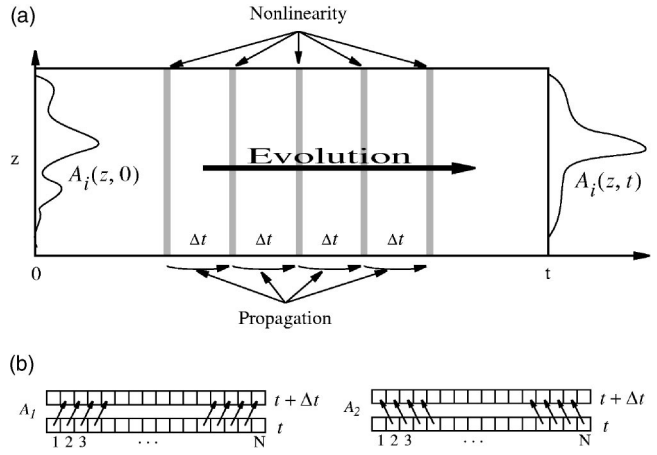

FIG. 3. The split-step method. (a) The actions of the propagation and the nonlinearity operators are split in time; (b) the action of the propagation operator for $\Delta z = c\Delta t/n$ is equivalent to a shift in the discretization bins for the two fields (A_1, laser; A_2, Stokes).

gation distance $c\Delta t/n$. In this case, the propagation operator introduces shifts $z \pm c\Delta t/n = z \pm \Delta z$ in the spatial coordinate of the fields and is easy to calculate [see Fig. 3(b)]. Following this split-action procedure, the solution of Eqs. (1) is obtained numerically. The only complication arises from the fact that in order to achieve reasonable accuracy, the discretization step Δz has to be small, leading to an increased memory use for storage of all past values of the product $A_1(z,t_n)A_2^*(z,t_n)$ necessary for the computation of the coupling integral (1c). It is sufficient to keep the history approximately $10\tau_p$ long in order to achieve an optimum speed/accuracy ratio.

In Eqs. (1), a spontaneous Brillouin scattering term is not included. Therefore, the numerical method described above, applied for the system (1), is capable of predicting the evolution of both laser and Stokes fields, provided the Stokes signal is initially seeded. In the following, we present an extension to the split-step method, which accounts for the spontaneous scattering of the pump field, thus providing a tool for modeling the behavior of an SBS pulse compressor with no assumed parameters in the fully transient regime.

The initiation of SBS from noise has been the subject of many theoretical [11,12] and experimental [13–15] investigations. At present, there are two complementary trends in the description of the early stages of amplification. In the distributed fluctuating source approach [11], a Langevin noise term $f(z,t)$ is added to the right-hand side of Eq. (1c),

$$Q(z,t) = \frac{1}{\sqrt{2\pi}} \int_{-\infty}^{t} g(t-\tau)[A_1(z,\tau)A_2^*(z,\tau) + f(z,\tau)]d\tau.$$

For a laser beam with cross section A, traversing a Brillouin-active medium with temperature T, unperturbed density ρ_0, sound velocity v, and sound damping parameter Γ (different from the Brillouin linewidth Γ_B [16]), this both spatially and temporally δ-correlated Gaussian random term with zero mean [$\langle f(z,t)\rangle = 0$] is characterized by the following relation:

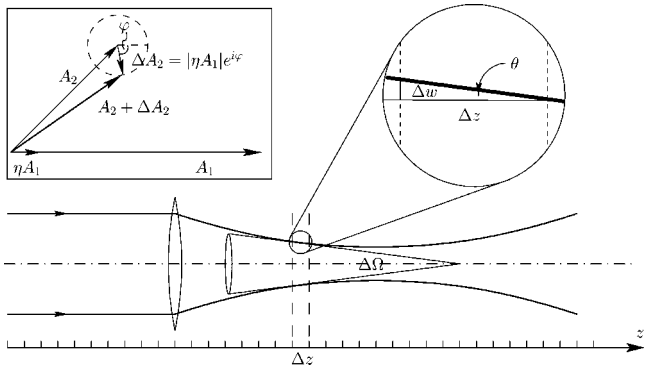

FIG. 4. A vector diagram of the spontaneous scattering contribution to the Stokes signal. At any particular position in space, the scattered field $\eta A_1(z)$ is added to the Stokes component A_2 with an arbitrary phase $\varphi \in (0, 2\pi)$.

$$\langle f(z',t')f^*(z'',t'')\rangle = Q\delta(z'-z'')\delta(t'-t''), \tag{4}$$

where $Q = 2kT\rho_0\Gamma/(v^2 A)$ is the fluctuation strength parameter. A noise term with these properties [Eq. (4)] has been successfully used for modeling and accurate determination of the intensity [11] and phase [17] fluctuations in both bulk media and fibers [15].

In an alternative approach [12], the spontaneously scattered light, rather than the density fluctuations, is taken as the initiation source. In this model, the known differential cross section per unit volume for scattering from thermal fluctuations [18] is used,

$$R_B = \frac{1}{V}\frac{d\sigma}{d\Omega} = \frac{\pi^2 kT}{2\lambda^4 \rho_0 v^2}\gamma^2, \tag{5}$$

where γ is the electrostriction constant of the medium. The spatial distribution of the spontaneous noise along the propagation axis is then

$$|\Delta A_2(z)|^2 = R_B \Delta\Omega(z)\Delta z |A_1(z)|^2 = \eta(z)^2 |A_1(z)|^2, \tag{6}$$

where $\eta(z)^2 = R_B\Delta\Omega(z)\Delta z$ is the total scattering coefficient for a particular point in space z.

All parameters in the definition of $\eta(z)$ are known quantities for any specific experimental setup. The solid angle $\Delta\Omega(z)$ subtended by the interaction volume is calculated for each position in space z according to the sketch in Fig. 4. Spontaneously scattered light with wave vectors outside the cone, with solid angle $\Delta\Omega(z)$, will leave the interaction region and therefore will not contribute to the noise. For every spatial bin $(z, z+dz)$ in our model, the spontaneously scattered signal $\Delta A_2(z)$ calculated using Eq. (6) adds to the Stokes field with an arbitrary phase $\varphi \in (0, 2\pi)$, as depicted in the inset of Fig. 4. This flat phase probability distribution of the spontaneously scattered light reflects the physical situation. In any realistic model, the spatial bin size is much larger than the wavelength of the optical field, and the step in time is much larger than the light period. Therefore, the phase of the spontaneously scattered light will be completely random, corresponding to an arbitrary creation time of the spontaneously scattered photons.

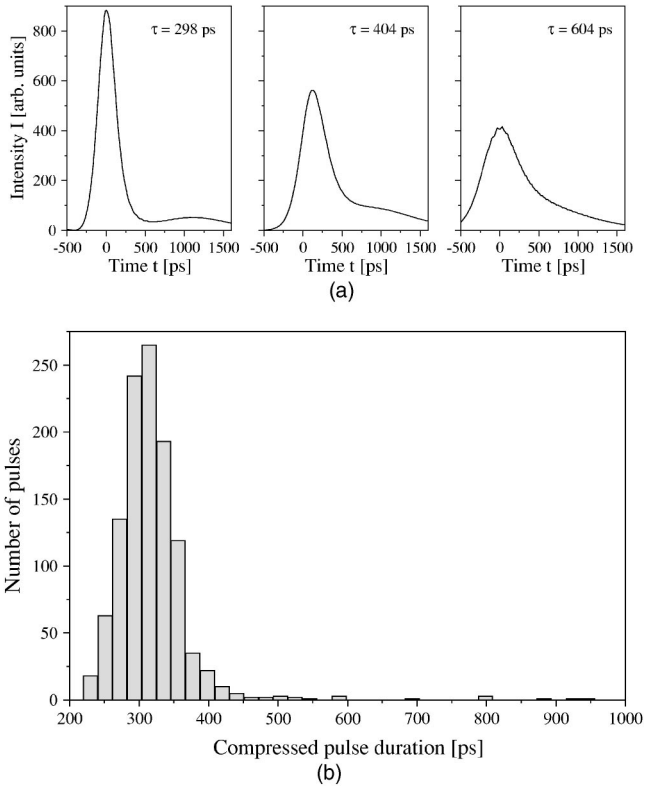

FIG. 5. Numerical results. (a) Three outcomes of SBS pulse compression with spontaneous noise source included; (b) a histogram of the compressed pulse durations.

The introduction of a physically correct spontaneous noise source in Eqs. (1) is only possible if the full three-dimensional beam distribution is considered. In the case of a SBS generator-amplifier geometry, however, the transverse field evolution is analytically known [19] (focused Gaussian pump beam) and can be used for calculation of $\Delta\Omega(z)$ at each step. In this way, the dimensionality of the system (1) can be kept low (z,t), allowing us to apply the efficient split-step method even in the more complex case of noise initiation of the Stokes signal. The calculations are performed with beam parameters matching the following experimental conditions: initial pump beam width of 1 cm, focused by a lens ($f=10$ cm) in water at $T=300$ K.

Using the model described above, with a spontaneous noise source included, the outcome of every simulation run yields a different pulse shape, thus reproducing a "real" experiment. In Fig. 5(a), three compressed pulses are shown with durations ranging from 298 to 604 ps. A comparison with the experimentally observed compressed pulses [Fig. 2(a)] confirms the presence of a tail more than 1 ns long, as well as a broad pulse-width distribution. In Fig. 5(b), the histogram of the compressed pulse durations for 1127 runs is shown. The mean of the distribution is at 310 ps with a standard deviation of 35 ps. This result is in excellent agreement with the experimentally obtained values [see Fig. 2(b)] and serves as a validation for our model.

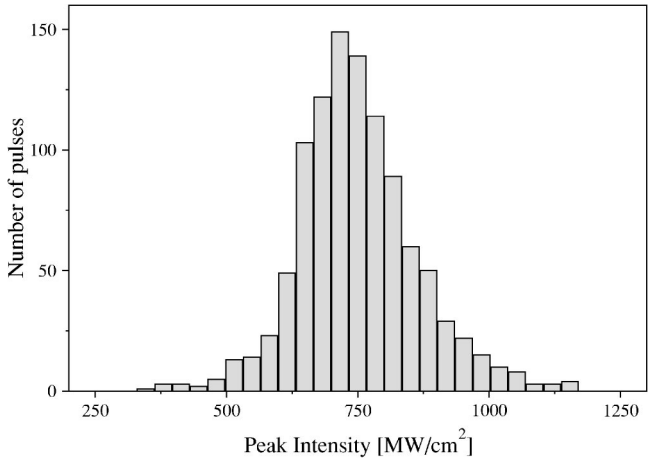

FIG. 6. A histogram of the peak intensity after SBS pulse compression.

The pulse duration spread naturally results in pulse-to-pulse fluctuations of the peak intensity. From the relevant histogram, presented in Fig. 6, an average peak intensity $\bar{I}=734$ MW/cm^2 is deduced along with the standard deviation of 95 MW/cm^2. For a beam of 1 cm width and average pulse duration of 310 ps, the average energy in the compressed pulse can be estimated at $\bar{E}=275$ mJ. Consequently, the expected reflectivity of the SBS pulse compressor is $\approx$92%. In this efficiency estimation, only the energy in the main compressed pulse is considered. The remaining 8% of the energy is "lost" in the tail of the scattered pulse, as well as in transmission of the front portion of the pump pulse, which passes through the focus before SBS threshold is reached. These two loss mechanisms have to be considered when an SBS pulse compressor is designed. Proper balance between input beam diameter and focal length of the lens must be achieved in order to minimize both pump transmission and "tail" contribution. In this regard, the model presented here has the potential to serve as a design optimization tool as well.

IV. CONCLUSIONS

We have introduced a fully transient model of SBS with a distributed spontaneous scattering noise source. Using this model, we have accurately predicted the compressed pulse duration, peak intensity, and reflectivity of a generator-amplifier setup. Although noise initiation of SBS is well understood and extensively discussed in the literature, our implementation of distributed noise in *transient* stimulated Brillouin scattering pulse compression allows a unique access to the time scale of the order of the phonon lifetime. In this temporal domain, the randomness of the initiation of the SBS process is experimentally detected as macroscopic pulse-to-pulse fluctuations. Most importantly, our model accurately reproduces the statistical distribution of pulse durations measured in an experiment and is now being successfully used for the design of improved and more efficient pulse compressor solutions.

[1] M. Maier, W. Kaiser, and J. A. Giordmaine, Phys. Rev. Lett. **17**, 1275 (1966).
[2] D. T. Hon, Opt. Lett. **5**, 516 (1980).
[3] F. Brandi, D. Neshev, and W. Ubachs, Phys. Rev. Lett. **91**, 163901 (2003).
[4] Z.-S. Li, J. Norin, A. Persson, C.-G. Wahlström, S. Svanberg, P. S. Doidge, and E. Biémont, Phys. Rev. A **60**, 198 (1999).
[5] P. A. C. Jansson, B. A. M. Hansson, O. Hemberg, M. Otendal, A. Holmberg, J. de Groot, and H. M. Hertz, Appl. Phys. Lett. **84**, 2256 (2004).
[6] I. Velchev, D. Neshev, W. Hogervorst, and W. Ubachs, IEEE J. Quantum Electron. **35**, 1812 (1999).
[7] C. B. Dane, W. A. Newman, and L. A. Hackel, IEEE J. Quantum Electron. **30**, 1907 (1994).
[8] S. Schiemann, W. Ubachs, and W. Hogervorst, IEEE J. Quantum Electron. **33**, 358 (1997).
[9] D. Neshev, I. Velchev, W. Majewski, W. Hogervorst, and W. Ubachs, Appl. Phys. B: Lasers Opt. **68**, 671 (1999).
[10] M. J. Damzen and H. Hutchinson, IEEE J. Quantum Electron. **19**, 7 (1983).
[11] R. W. Boyd, K. Rzążewski, and P. Narum, Phys. Rev. A **42**, 5514 (1990).
[12] N.-M. Nguyen-Vo and S. J. Pfeifer, IEEE J. Quantum Electron. **29**, 508 (1993).
[13] V. I. Bespalov, A. A. Betin, G. A. Pasmanik, and A. A. Shilov, JETP Lett. **31**, 630 (1980).
[14] E. M. Dianov, A. Y. Krasik, A. V. Luchnikov, and A. K. Senatorov, Sov. J. Quantum Electron. **19**, 508 (1989).
[15] A. L. Gaeta and R. W. Boyd, Phys. Rev. A **44**, 3205 (1991).
[16] R. W. Boyd, *Nonlinear Optics* (Academic Press, San Diego, 2003).
[17] S. Afshaarvahid, V. Devrelis, and J. Munch, Phys. Rev. A **57**, 3961 (1998).
[18] A. Einstein, Ann. Phys. **33**, 1275 (1910).
[19] H. Kogelnik and T. Li, Appl. Opt. **5**, 1550 (1966).